AIP | The Journal of Chemical Physics

Theoretical and experimental studies of CIDNP kinetics in recombination of radical pairs by the method of switched external magnetic field. III. Free radicals in homogeneous solution

M. V. Fedin, E. G. Bagryanskaya, P. A. Purtov, T. N. Makarov, and H. Paul

Citation: The Journal of Chemical Physics **117**, 6148 (2002); doi: 10.1063/1.1502650
View online: http://dx.doi.org/10.1063/1.1502650
View Table of Contents: http://scitation.aip.org/content/aip/journal/jcp/117/13?ver=pdfcov
Published by the AIP Publishing

Theoretical and experimental studies of CIDNP kinetics in recombination of radical pairs by the method of switched external magnetic field. III. Free radicals in homogeneous solution

M. V. Fedin and E. G. Bagryanskaya
International Tomography Center SB RAS, Novosibirsk, 630090, Russia

P. A. Purtov
Institute of Chemical Kinetics and Combustion SB RAS, Novosibirsk, 630090, Russia

T. N. Makarov and H. Paul
Physical-Chemistry Institute, University of Zurich, CH-8097 Zurich, Switzerland

(Received 16 April 2002; accepted 2 July 2002)

The method of chemically induced dynamic nuclear polarization in a switched external magnetic field (SEMF CIDNP) is applied here for the first time to an experimental study of short-lived neutral radicals in homogeneous solutions. With three photochemical reactions it is exemplified, that SEMF CIDNP allows investigations of the kinetics of the transient species with high time-resolution as well as a determination of their spin relaxation times in low magnetic fields. A theoretical approach is developed, which permits simulation and analysis of the experimental data. In weak magnetic fields (0.5–2.0 mT) the effective spin-lattice relaxation times for the decay of the chemically induced spin polarizations in benzyl, tert-butyl, and 2-hydroxy-2-propyl radicals are found to be $T_1=(3.8\pm0.5)$ μs, $T_1=(7.8\pm0.5)$ μs, and $T_1=(2.5\pm0.5)$ μs, respectively, in benzene solution at room temperature. They are in fair agreement with relaxation times determined by time-resolved *X*-band electron paramagnetic resonance spectroscopy at strong magnetic fields ($\approx$350 mT).
 [DOI: 10.1063/1.1502650]

I. INTRODUCTION

The method of chemically induced dynamic nuclear polarization in a switched external magnetic field (SEMF CIDNP) has been suggested theoretically by Michailov *et al.*,[1] and then a number of theoretical and experimental studies have been concerned with this new technique.[2–4] SEMF CIDNP involves an abrupt field switching during the lifetime of radical intermediates. In this method, after initiating a reaction with a laser pulse, CIDNP is formed during a variable time delay t_0 in a first magnetic field B_1, and then, after switching, CIDNP formation continues in a second field B_2 during a fixed time $\Delta\tau$. Finally the magnetic field is switched back to B_1. The resulting nuclear polarization is monitored by taking NMR spectra at time delays much longer than the lifetimes of the radical intermediates. The t_0-dependence of the CIDNP is called the SEMF CIDNP kinetics. As has been shown in Ref. 4, the SEMF CIDNP kinetics of radical pairs (RPs) in micellar solution reflects the kinetics of their recombination and allows their investigation with high time-resolution. In Ref. 3 the SEMF CIDNP technique has been used to measure the rate of degenerate electron exchange in systems containing ion-radical pairs.

Up to now, the method has not yet been applied to study reactions of short-lived neutral radicals in homogeneous solutions, and this work aims at an examination of the information one can gain for such systems. One may imagine two possible contributions to the influence the SEMF has on the CIDNP of the products. The first one is caused by the influence of the field switch on the CIDNP generated in RPs. Since CIDNP is magnetic field dependent, the variation of the t_0-delay leads to a change in the ratio of the RPs in which the polarization was formed in B_1 and in B_2, and thus to a change of the total CIDNP signal measured. In this case it is reasonable to expect that the SEMF CIDNP kinetics should reflect the kinetics of the RP recombination. The second possible contribution may result from the influence the SEMF has on the CIDNP in free radicals due to electron–nuclear polarization transfer, which in low magnetic fields takes place under both adiabatic[3,5] and nonadiabatic[3] field switching conditions. The low-field eigenfunctions depend on the magnetic field via the mixing coefficients. Therefore, the spin polarization will be different before and after the field switching.[3] In case of this contribution one would expect the SEMF CIDNP kinetics to be determined by both the chemical decay of the radicals and their spin relaxation times.

Thus, the main purpose of the present work was to apply the SEMF CIDNP technique to reactions of neutral radicals in homogeneous solution, in order to clarify the roles played by the two contributions mentioned above, and to explore which kind of quantitative information can be gained about the radicals and RPs. For comparison with the SEMF CIDNP results in weak magnetic fields, we have also determined the radical electron spin relaxation times in a strong magnetic field (350 mT) using *X*-band time-resolved electron paramagnetic resonance spectroscopy (TR EPR).

II. THEORY

In order to understand the main features of SEMF CIDNP if applied to neutral radicals in homogeneous solu-

tion we consider theoretically the simplest case of a radical, $A\bullet$, possessing only one magnetic nucleus. Assume that the photochemical reaction proceeds via the scheme,

$$M \rightarrow A\bullet + \bullet B,$$

$$A\bullet + \bullet A \xrightarrow{2k} AA, \tag{i}$$

$$A\bullet + \bullet B \xrightarrow{2k} AB, \tag{ii}$$

$$B\bullet + \bullet B \xrightarrow{2k} BB. \tag{iii}$$

The Liouville equation for the density matrix ρ_A of radical A can then be written in the form,[6]

$$\frac{\partial \rho_A}{\partial t} = (i\hat{\hat{L}}_A + \hat{\hat{R}}_A)\rho_A(t) - [A]_0 \hat{\hat{K}}^A(t)\rho_A(t) \otimes \rho_A(t) - [B]_0 \hat{\hat{K}}^B(t)\rho_B(t) \otimes \rho_A(t), \tag{1}$$

where the operators $\hat{\hat{L}}_A$ and $\hat{\hat{R}}_A$ describe the spin dynamics and relaxation of the diffusing radical A, and $\hat{\hat{K}}^A$ and $\hat{\hat{K}}^B$ the spin dynamics of radicals A and B during their encounter. For the calculations which follow Eq. (1) can be rewritten in a more convenient form,

$$\frac{\partial \rho_A}{\partial t} = (i\hat{\hat{L}}_A + \hat{\hat{R}}_A)\rho_A - [A]_0 f_A(t)\hat{\hat{K}}^{AA}\rho_A - [B]_0 f_B(t)\hat{\hat{K}}^{BA}\rho_A. \tag{2}$$

The second and third terms on the right-hand side of the equation describe the chemical decay of the radicals $[A]_0 = [B]_0 \equiv R_0$ are the initial concentrations and $f_A(t)$ and $f_B(t)$ describe the time dependencies of the concentrations of the radicals A and B, respectively. $\hat{\hat{K}}^{AA}$ and $\hat{\hat{K}}^{BA}$ are given by

$$\hat{\hat{K}}^{AA} = \hat{\hat{K}}_r^{AA} + \hat{\hat{K}}_j^{AA}, \quad \hat{\hat{K}}^{BA} = \hat{\hat{K}}_r^{BA} + \hat{\hat{K}}_j^{BA}, \tag{3}$$

where the matrices $\hat{\hat{K}}_r^{AA}$ and $\hat{\hat{K}}_r^{BA}$ describe the chemical decay of the radicals in the reactions (i) and (ii), respectively, and the matrices $\hat{\hat{K}}_j^{AA}$ and $\hat{\hat{K}}_j^{BA}$ describe the formation of polarization in radical F-pairs.

The CIDNP of the products AA and AB, corresponding to a switch from B_1 to B_2 after a time delay t_0, is given by

$$P_{AA}(t_0) = R_0\left[\hat{\hat{I}}(B_1)\cdot\hat{\hat{K}}_r^{AA}\int_0^{t_0} f_A(t)\rho_A(B_1,t)dt + \hat{\hat{I}}(B_2)\cdot\hat{\hat{K}}_r^{AA}\int_{t_0}^{\infty} f_A(t)\rho_A(B_2,t)dt\right],$$

$$P_{AB}(t_0) = R_0\left[\hat{\hat{I}}(B_1)\cdot\hat{\hat{K}}_r^{BA}\int_0^{t_0} f_B(t)\rho_A(B_1,t)dt + \hat{\hat{I}}(B_2)\cdot\hat{\hat{K}}_r^{BA}\int_{t_0}^{\infty} f_B(t)\rho_A(B_2,t)dt\right], \tag{4}$$

where $\hat{\hat{I}}(B_{1,2})$ is the projection operator on the nuclear spin states in the magnetic fields B_1 and B_2. For simplicity we assume the duration of the B_2 field application to be much longer than the radical lifetimes and do not take into account the switch back to B_1. We also assume the magnetic field switching to be adiabatic, what is correctly accounted for by the boundary condition $\rho_A(B_1,t_0) = \rho_A(B_2,t_0)$.

The formal solution of Eq. (2) can be written as

$$\rho_A(t) = \exp\left(\int_0^t ((i\hat{\hat{L}}_A + \hat{\hat{R}}_A) - R_0 f_A(t')\hat{\hat{K}}^{AA} - R_0 f_B(t')\hat{\hat{K}}^{BA})dt'\right)\cdot\rho_0. \tag{5}$$

Designating $i\hat{\hat{L}}_A + \hat{\hat{R}}_A \equiv \hat{\hat{A}}$, and $R_0 f_A(t)\hat{\hat{K}}^{AA} + R_0 f_B(t)\hat{\hat{K}}^{BA} \equiv \hat{\hat{B}}$, and assuming the commutator $[\hat{\hat{A}},\hat{\hat{B}}] \equiv 0$ (we will show later under which condition this approximation holds), expression (5) can be rewritten as

$$\rho_A(t) = \hat{\hat{T}}(t)\exp\left(-R_0\hat{\hat{K}}^{AA}\int_0^t f_A(t')dt' - R_0\hat{\hat{K}}^{BA}\int_0^t f_B(t')dt'\right)\cdot\rho_A(0), \tag{6}$$

where

$$\hat{\hat{T}}_A(t) = \exp((i\hat{\hat{L}}_A + \hat{\hat{R}}_A)t) \tag{7}$$

is the operator of spin evolution.

Let $f_A(t) = f_B(t) = 1/(1+2kR_0t)$, what obviously is applicable for the reaction scheme used and for an only weak influence of the spin transitions during the encounters of the reagents. Then, Eq. (6) is brought to

$$\rho_A(t) = \hat{\hat{T}}(t)\left(\frac{1}{1+2kR_0t}\right)^{(\hat{\hat{K}}^{AA}+\hat{\hat{K}}^{BA})/2k}\cdot\rho_A(0). \tag{8}$$

Thus, the problem is reduced to the calculation of the spin evolution operator $\hat{\hat{T}}(t)$, i.e., to the solution of the equation,

$$\frac{\partial \rho_A}{\partial t} = (i\hat{\hat{L}}_A + \hat{\hat{R}}_A)\rho_A. \tag{9}$$

Let us discuss specifically the matrices used. For clarification of the main features it is sufficient to operate in the Liouville basis of populational elements of the density matrix $|1,1\rangle$, $|2,2\rangle$, $|3,3\rangle$, $|4,4\rangle$, where $|1\rangle$, $|2\rangle$, $|3\rangle$, $|4\rangle$ are the eigenfunctions of the radical with the magnetic nucleus. They are obtained from the Breit–Rabi expressions,

$$|1\rangle = |\alpha_e\alpha_n\rangle, \quad E_1 = \frac{\omega_e}{2} + \frac{a}{4},$$

$$|2\rangle = C_1|\alpha_e\beta_n\rangle + C_2|\beta_e\alpha_n\rangle, \quad E_2 = -\frac{a}{4} + \frac{\sqrt{\omega_e^2+a^2}}{2},$$

$$|3\rangle = |\beta_e\beta_n\rangle, \quad E_3 = -\frac{\omega_e}{2} + \frac{a}{4}, \tag{10}$$

$$|4\rangle = C_2|\alpha_e\beta_n\rangle - C_1|\beta_e\alpha_n\rangle, \quad E_4 = -\frac{a}{4} - \frac{\sqrt{\omega_e^2+a^2}}{2},$$

$$C_1^2 = \frac{1}{2}\left(1 + \frac{\omega_e}{\sqrt{\omega_e^2+a^2}}\right), \quad C_2^2 = \frac{1}{2}\left(1 - \frac{\omega_e}{\sqrt{\omega_e^2+a^2}}\right).$$

Here a is the HF1-constant, ω_e the magnetic field, and the subscripts e and n correspond to electron and nucleus, respectively.

We introduce the effective time of low-field spin relaxation T_1 phenomenologically in a relaxation matrix $\hat{R}$, which reads in the basis chosen,

$$\hat{\hat{R}}=\frac{1}{4T_1}\times\begin{bmatrix}-3 & 1 & 1 & 1\\ 1 & -3 & 1 & 1\\ 1 & 1 & -3 & 1\\ 1 & 1 & 1 & -3\end{bmatrix}. \tag{11}$$

It is assumed that the relaxation rate is equal between all four spin levels. Since the efficiency of S–T transitions during the radical encounters is small, the matrices $\hat{\hat{K}}_r$ and $\hat{\hat{K}}_j$ in the same basis are

$$\hat{\hat{K}}_r^{AA}=\hat{\hat{K}}_r^{BA}=\begin{bmatrix}k & 0 & 0 & 0\\ 0 & k & 0 & 0\\ 0 & 0 & k & 0\\ 0 & 0 & 0 & k\end{bmatrix},$$
$$\hat{\hat{K}}_j^{AA}=\hat{\hat{K}}_j^{BA}=\begin{bmatrix}\theta_1 & 0 & 0 & 0\\ 0 & \theta_2 & 0 & 0\\ 0 & 0 & \theta_3 & 0\\ 0 & 0 & 0 & \theta_4\end{bmatrix}, \tag{12}$$

where k is the radical recombination rate and the $\theta_i \ll k$ characterize the CIDNP formation in radical F-pairs. The condition $\theta_i \ll k$ means, that the matrices $\hat{\hat{K}} \equiv \hat{\hat{K}}_r + \hat{\hat{K}}_j$ and, consequently, the matrix $\hat{\hat{B}}$ are almost proportional to the unit matrix. Thus the approximation $[\hat{A},\hat{B}] \cong 0$ suggested earlier is well applicable.

Equation (9) has been solved using the Laplace transformation,

$$s\tilde{\rho}(s)-\rho(t=0)=(-i\hat{\hat{L}}+\hat{\hat{R}})\tilde{\rho}(s)$$
$$\Rightarrow \tilde{\rho}(s)=[i\hat{\hat{L}}-\hat{\hat{R}}+s\hat{\hat{E}}]^{-1}\rho(t=0), \tag{13}$$

where $\tilde{\rho}(s)$ is the Laplace image of the density matrix and $\hat{\hat{E}}$ the unit matrix. For calculation of $\rho(t)$ the inverse Laplace transformation and matrix inversion have then been carried out numerically. The parameters of the calculation were B_0, B_1, a, k, R_0, θ_i, T_1 and the initial populations of the radical spin levels n_i.

Figures 1(a) and 1(b) show the SEMF CIDNP kinetics calculated for two different cases corresponding to zero [Fig. 1(a), $\theta_i=0$] and significant [Fig. 1(b), $\theta_i \neq 0$] CIDNP formation in radical F-pairs in comparison with the geminate polarization. In both cases the kinetics has been calculated for different ratios of the second-order decay rate $2kR_0$ and the relaxation rate $1/T_1$ taken as 10^6 s^{-1}. As one can see from Fig. 1(a), in the case $\theta_i=0$ the kinetics does not depend on R_0 at $1/T_1 \gg 2kR_0$ and shows there a monoexponential decay with time-constant $T_1=1$ μs, which is in complete agreement with the exact solution of equation $\partial\rho/\partial t=\hat{\hat{R}}\rho$. When $1/T_1 \sim 2kR_0$, the kinetics deviates from the monoexponential decay and depends noticeably on R_0 due to the contribution

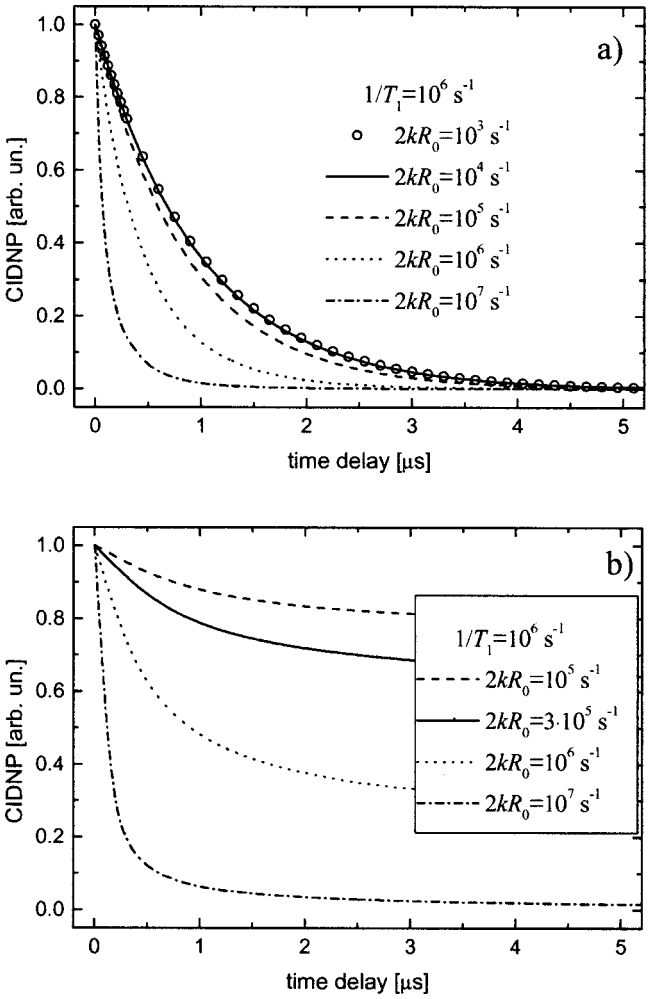

FIG. 1. SEMF CIDNP kinetics calculated using the solution of Liouville equation for the radical with one magnetic nucleus. The following set of parameters has been used in calculations: $T_1=1$ μs, $2kR_0$ as shown in the figure, $B_1=0.5$ mT, $B_2=7.5$ mT, $a=5$ mT, initial populations of radical spin levels $n_1=1$, $n_2=0.05$, $n_3=n_4=0$, $\theta_i=0$ in (a) and $\theta_{i\neq4}=0$, $\theta_4=0.01$ in (b).

of the second-order decay. In the limiting case $1/T_1 \ll 2kR_0$ the kinetics follows the second-order decay law $1/(1+2kR_0t)$ and the contribution of the relaxation becomes negligible. In the case $\theta_i \neq 0$, shown in Fig. 1(b), the kinetics depends on R_0 for all ratios between $1/T_1$ and $2kR_0$ and is determined by both spin relaxation and chemical reaction. Consequently, we conclude that in case of only small F-pair CIDNP contributions and sufficiently slow chemical decay the SEMF CIDNP kinetics is determined by the spin relaxation, whereas in other cases it contains contributions from both relaxation and chemical kinetics.

The above consideration is helpful to understand the main features of SEMF CIDNP, but it is applicable only for radicals following the simple reaction schemes (i)–(iii) with one species possessing a single hyperfine interacting nucleus. For the analysis of experimental data obtained in more complex chemical reactions, yielding radicals with numerous HFI constants, we have taken the kinetic approach developed by Vollenweider *et al.*[7] for high-field time-resolved CIDNP and have modified it for our low-field condition.

Assume that a photochemical reaction proceeds via the following scheme, applicable for the photolysis of many symmetrical ketones,

$$R\text{–C(O)–}R \rightarrow R\text{–CO}\bullet + \bullet R \overset{2k}{\rightarrow} R\text{–C(O)–}R,$$

$$R\text{–CO}\bullet \overset{k_{CO}}{\rightarrow} R\bullet + \text{CO}\uparrow, \qquad \text{(j)}$$

$$R\bullet + \bullet R \overset{2k}{\rightarrow} R\text{–}R, \qquad \text{(jj)}$$

$$R\text{–CO}\bullet + \bullet\text{CO–}R \overset{2k}{\rightarrow} R\text{–C(O)–C(O)–}R. \qquad \text{(jjj)}$$

The kinetic equations for the nuclear polarizations of the radicals $R\bullet(P^R)$ as well as the products $R\text{–}R$ and $R\text{–C(O)–}R \equiv \text{M}$ (P^{RR} and P^M) can be extended for low magnetic fields by accounting in addition also for the CIDNP formed in the symmetrical radical pairs $[R\bullet\bullet R]$,

$$\begin{aligned}\frac{\partial P^R}{\partial t} &= -2k[R]P^R - 2k[RCO]P^R \\ &\quad - 2k[R]^2\chi - 2k[R]\cdot[RCO]\xi - \frac{P^R}{T_1}, \\ \frac{\partial P^{RR}}{\partial t} &= 2k[R]P^R + 2k[R]^2\chi, \\ \frac{\partial P^M}{\partial t} &= 2k[RCO]P^R + 2k[R]\cdot[RCO]\xi.\end{aligned} \qquad (14)$$

Here, $[R]$ and $[RCO]$ are the concentrations of the radicals R and RCO, and χ and ξ are the coefficients describing the efficiency of CIDNP formation per collision in the RPs $[R\bullet\bullet R]$ and $[R\bullet\bullet RCO]$, respectively. For the high-field time-resolved CIDNP T_1 is introduced as the nuclear relaxation time. Under our conditions of low magnetic field the relaxation transitions between the radical spin levels are neither purely nuclear nor electronic. Thus, T_1 in Eq. (14) just describes the electron–nuclear relaxation time of the spin polarization.

As the coefficients χ and ξ are magnetic field dependent, the integration of Eqs. (14) has to account for the field switching procedure in the SEMF CIDNP experiment by taking

$$\begin{cases} 0<t<t_0 & \chi_1,\xi_1 \\ t_0<t<t_0+\Delta\tau & \chi_2,\xi_2 \\ t_0+\Delta\tau<1<\infty & \chi_1,\xi_1 \end{cases} \qquad (15)$$

with $\chi_{1,2}=\chi(B_{1,2})$, $\xi_{1,2}=\xi(B_{1,2})$, and $\Delta\tau$ being the duration of the B_2 field application. In addition, the polarization transfer occurring under magnetic field switching conditions has to be accounted for by the boundary conditions,

$$P^R|_{t_0,B_2} = P^R|_{t_0,B_1}\times(1+\Delta P^R)$$

and

$$P^R|_{t_0+\Delta\tau,B_1} = P^R|_{t_0+\Delta\tau,B_2}/(1+\Delta P^R), \qquad (16)$$

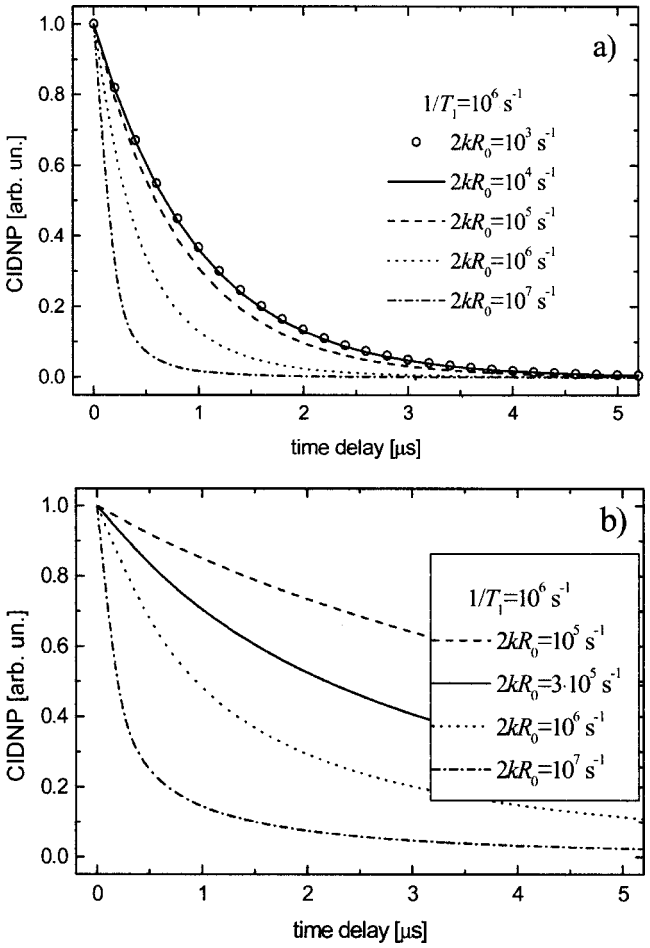

FIG. 2. SEMF CIDNP kinetics calculated using the modified kinetic approach for the following set of parameters: $T_1=1$ μs, $2kR_0$ as shown in the figure, $\Delta\tau=5$ μs, $\Delta P^R=0.1$, $\chi_i,\xi_i=0$ in (a), and in $\chi_2=\xi_2=2\chi_1=2\xi_1=10\cdot P_0^R/R_0$.

where ΔP^R is a dimensionless phenomenological parameter characterizing the polarization change because of the magnetic field switching. Thus, the simulation of the SEMF CIDNP kinetics of the more realistic chemical scheme (j)–(jjj) now involves the parameters χ_1, ξ_1, χ_2, ξ_2, $\Delta\tau$, ΔP^R, T_1, $2k$, the initial concentrations of the radicals $[R]_0=[RCO]_0\equiv R_0$, and the geminate polarization, i.e., $P^R(t=0)\equiv P_0^R$.

The parameters χ_1, ξ_1, χ_2, ξ_2 correspond with the θ_i and characterize the CIDNP formed in radical F-pairs. Figure 2(a) shows the SEMF CIDNP kinetics calculated for the case that all $\chi_i,\xi_i=0$, i.e., when no polarization is formed in diffusional RPs. One can see that in this case the kinetic curves are just identical with those shown in Fig. 1(a). The parameters $\Delta\tau$, ΔP^R, and P_0^R influence only the amplitude of the kinetics, and the significant parameters for the decay are T_1 and $2kR_0$. Figure 2(b) represents the opposite case of a large polarization formed in F-pairs as compared with P_0^R, i.e., $\chi_i,\xi_i\neq0$; $\chi_i,\xi_i\gg P_0^R/R_0$. One can see that the accordance with the exact calculation shown in Fig. 1(b) is not so good, but the qualitative features are well reproduced. The differences are explained by the different accounts of relaxation. In the kinetic approach the spin relaxation is involved as monoexponential decay of CIDNP, while in the correct calculation the relaxation does not necessarily lead to a polar-

ization decay. Note, that this difference becomes significant only in the case $1/T_1 \ll 2kR_0$.

Thus, the above consideration shows the abilities of SEMF CIDNP for measurements of spin relaxation times in low magnetic field. The limitation for the shortest measurable T_1 is determined by the time-resolution of the SEMF CIDNP setup. The limitation for the longest T_1 value depends on particular experimental conditions: on the one hand one should satisfy the condition $1/T_1 \gg 2kR_0$, but on the other side one must also obtain a sufficiently high CIDNP intensity.

III. EXPERIMENT

A. SEMF CIDNP

The experimental setup has been described elsewhere.[3,4] The solution was irradiated in a photochemical cell positioned in the magnetic field B_1 of an auxiliary magnet (0–70 mT) using UV light from an excimer laser (308 nm, 100 mJ, 10 Hz). After the laser and field pulses the sample was transferred into the probe of a Bruker Avance-200 NMR spectrometer, where the NMR spectra of the reaction products were detected. The transfer time was about 1 s. The external magnetic switching field B_s, parallel to B_1, was provided by Helmholz coils. The maximum B_s field amplitude was ± 7.0 mT, applied with a risetime of about 5 ns. The switch back to B_1 occurred after 2–5 μs within about 200 ns. An experimental time-jitter of about 20 ns existed between the laser pulse and the rise of the switching field and determined the time-resolution of our set-up. Note that this time is negligible on the time-scale of the kinetics involved.

B. TR EPR

The experimental set-up for time-resolved EPR measurements after laser flash photolytic radical generation has also been described previously.[8] It is comprised of an excimer laser Compex 102 (308 nm, 20 ns pulse width) and a cw-EPR detection system without field modulation (90 ns response time). Experiments were carried out at room temperature with benzene solutions. After deoxygenation by purging with helium (30–40 min), they were exposed to laser irradiation (0.3–5 mJ per pulse on sample surface, 10 Hz repetition rate) while slowly flowing (50–100 laser shots per irradiation volume) through a quartz cell (2 mm optical path length) inside a TE_{103} EPR cavity. Spectra and time profiles were recorded at microwave powers 0.1–80 mW. Steady-state EPR experiments were performed on a commercial EPR-spectrometer (Bruker EMX300).

IV. RESULTS AND DISCUSSION

Three photochemical reactions yielding alkyl radicals were chosen, namely, the photolyses of di-benzyl ketone (DBK), di-tert.butyl ketone (DTBK), and di-isopropylol ketone (DIPK) yielding benzyl ($PhCH_2$•), tert.butyl ($(CH_3)_3C$•), and 2-hydroxy-2-propyl radicals ($(CH_3)_2(OH)C$•), respectively. The photolysis of these ketones is well studied[9–13] and proceeds according to Scheme 1.

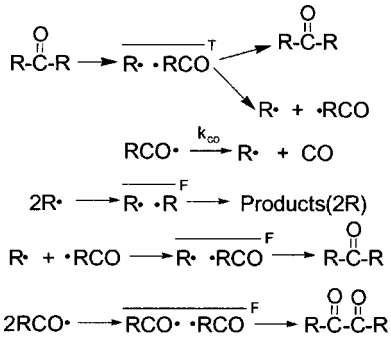

The main difference between the three ketones is the decarbonylation rate of the primarily formed acyl radicals. At room temperature in non-polar solutions they have been determined as $k_{CO} \sim 9 \cdot 10^6$ s^{-1} for $PhCH_2CO$•,[14] $k_{CO} \sim 5 \cdot 10^5$ s^{-1} for $(CH_3)_3CCO$•,[14] and $k_{CO} \sim 4 \cdot 10^7$ s^{-1} for $(CH_3)_2(OH)CCO$•.[15] Tert.butyl radicals have 9 protons with a HFI of 2.22 mT. In 2-hydroxy-2-propyl radicals the 6 methyl protons lead to a HFS of 1.95 mT and the OH-proton yields an additional splitting of 0.1 mT. The hyperfine structure of benzyl radicals consists of a HFI of $\approx$1.6 mT of the α-protons and HFI constants of 0.17–0.63 mT of the ortho, meta, and para ring protons.[16] All SEMF CIDNP experiments were carried out in magnetic fields B_1 of 0.5–2.0 mT, which are comparable to and lower than the values of the HFI constants of the radicals studied.

In the TREPR experiments the photolysis of benzyl-methyl ketone (BMK) and 2-hydroxy-2-methyl-propiophenone (HMP) were chosen as sources for benzyl and 2-hydroxy-2-propyl radicals, respectively, which are also well-studied photoreactions.[17,18]

Solutions. The concentrations used in the SEMF CIDNP experiments were 4–8 mM for DBK, 4–12 mM for DTBK, and 6 mM for DIPK. Initial BMK and HMP concentrations of 35 mM (o.d.=0.5) and 30 mM (o.d.=0.5) were used in all TREPR experiments. All compounds were used as purchased, only benzene was purified by distillation.

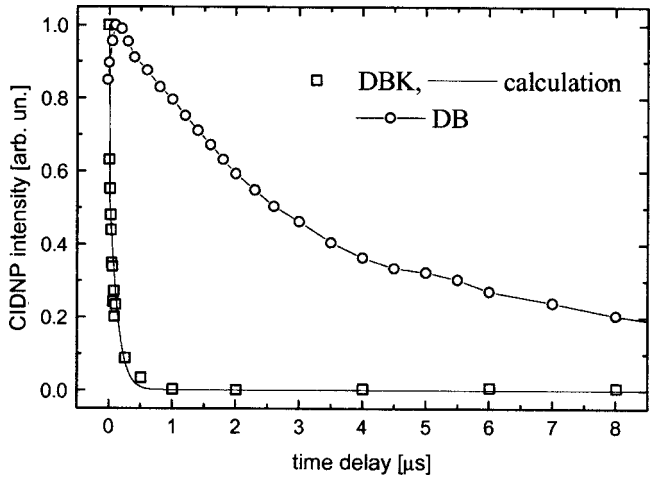

FIG. 3. SEMF CIDNP kinetics obtained during the photolysis of DBK by the NMR lines of DBK and dibenzyl (DB) in benzene. $B_1 = 2.0$ mT, $B_2 = 9.0$ mT, $\Delta\tau = 5$ μs.

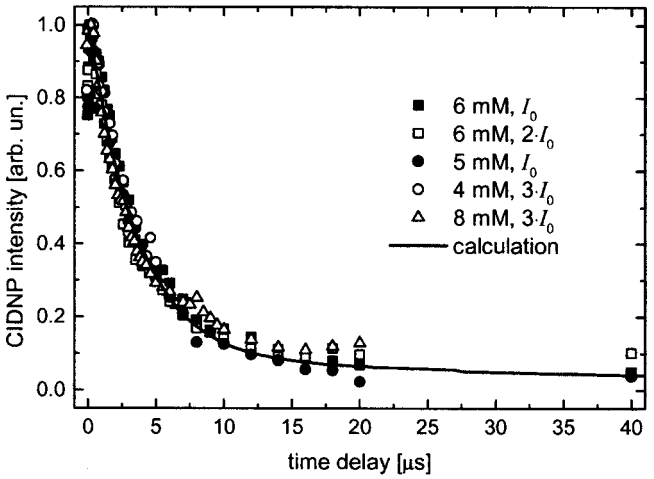

FIG. 4. SEMF CIDNP kinetics of DB measured at different initial concentrations of radicals R_0 in benzene. $B_1=2.0$ mT, $B_2=9.0$ mT, $\Delta\tau=5$ μs. The best fit to experimental curves has been obtained for $T_1=3.8$ μs, $\Delta P^R=1$, $\chi_1,\xi_1 \ll \chi_2=\xi_2=0.03 \cdot P_0^R/R_0$, $k_{co}=7 \cdot 10^6$ s^{-1}.

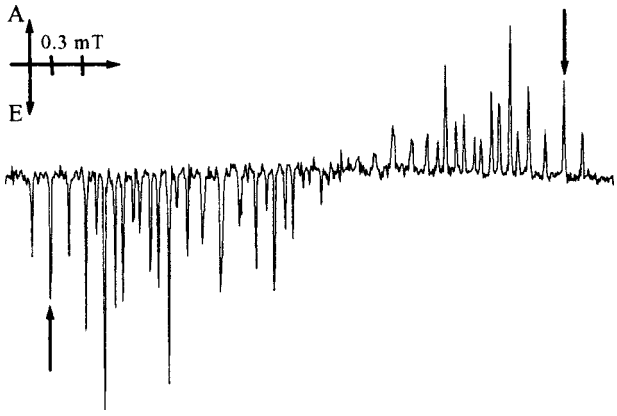

FIG. 5. TR EPR spectrum of benzyl radical recorded at time delay of 2.5 μs after laser excitation.

A. The photolysis of di-benzyl ketone

Figure 3 shows the SEMF CIDNP kinetics obtained during the photolysis of DBK in benzene. The detection was carried through on the NMR lines of the CH_2-protons of DBK and the reaction product dibenzyl (DB). The kinetics was measured in a magnetic field $B_1=2.0$ mT, switched to $B_2=9.0$ mT. The SEMF CIDNP kinetics obtained on the DBK protons is one order of magnitude faster than that on the DB protons and is determined by the decarbonylation of the phenacyl radical. It is well simulated with a decarbonylation rate constant $\sim 7 \cdot 10^6$ s^{-1}. The DB kinetics shows a decay on the microsecond time scale. Its short rise at the initial part is assigned to the geminate stage of reaction which, however, is obscured by the laser pulse duration and laser time-jitter.

Figure 4 shows the DB kinetics measured at different laser light intensities and concentrations of DBK, in order to vary the initial radical concentration R_0, which is determined by both laser pulse energy and optical density of the solution. One can see that the kinetics does not depend on R_0 within the experimental accuracy and, therefore, is determined by the spin relaxation in the radicals. Thus, a simulation using the kinetic approach allows us to obtain the spin relaxation time of the benzyl radicals, which is found to be $T_1=3.8\pm0.5$ μs. In this simulation the parameter $2kR_0$ has been taken small enough to provide independence of the kinetics on R_0. The other parameters are listed in the figure caption.

In order to check our result obtained for T_1 of benzyl radical in a low magnetic field (2 mT) we have measured T_1 also in a high magnetic field (300 mT) using TR EPR. After laser irradiation of benzyl-methyl ketone (BMK) in benzene solution, the EPR spectrum of benzyl radicals was observed (Fig. 5). As the photolysis of BMK occurs from an excited triplet state, the spectrum exhibits an E/A polarization pattern due to the RPM in the geminate radical pair. Two arrows in Fig. 5 mark a high- and low-field line positioned symmetrically to the center of the spectrum. Their overlap with neighboring resonances is negligibly weak and, therefore, their EPR time profiles have been chosen for our analysis.

To evaluate the relaxation times T_1 and T_2 of the benzyl radicals the procedure developed by Savitsky and Paul[19,20] was applied. In this method two different experiments are used. In the first one the quantity $\sigma_0=(1/2)\cdot(T_1^{-1}+T_2^{-1})$ is measured from Torrey oscillations of the TR EPR signal, the time dependence of which can be described by

$$V(t)=A\cdot\exp(-\sigma t)\sin(\omega_T t), \tag{17}$$

where the amplitude A is proportional to the initial radical concentration R_0, $\sigma=\sigma_0+k_{ex}[R_0]$, with k_{ex} being the Heisenberg spin exchange rate constant, $\omega_T=\sqrt{\omega_1^2-(1/4)\cdot(T_1^{-1}-T_2^{-1})^2}$ is the nutation frequency, which depends on the incident microwave power ω_1. In the second experiment T_2 is analyzed from the EPR linewidth.

The dependence of the EPR time profiles of the line pair (marked in Fig. 5 by arrows) on microwave power and laser light intensity was recorded. Clear oscillations were observed above 10 mW of incident microwave power. For each laser intensity at least four time profiles were taken in the oscillation limit and their Fourier spectra were fitted[19,20] to yield A, σ, ω_T. The dependence of the width σ of the nutation line in frequency space on its amplitude A is represented in Fig. 6. Linear regression in the region of small A yielded $\sigma_0=(2.25\pm0.40)\cdot10^5$ s^{-1}.

In order to get T_2 the line under investigation was measured by steady-state EPR. Low microwave powers were used to exclude saturation effects and additional line broadening. The analysis of the EPR linewidth yielded $\delta B_{1/2}=(2.6\pm0.5)$ mT. Using the expression for $\delta B=2/\gamma T_2$, the value of $T_2=(4.4\pm0.9)\cdot10^{-6}$ s was calculated. Since $\sigma_0^{-1}=(4.44\pm0.80)\cdot10^{-6}$ s is equal to T_2 within the error limits we have to assume that $T_1\approx T_2=(4.4\pm0.9)\cdot10^{-6}$ s.

Hence, we conclude that the relaxation time of benzyl radical measured by SEMF CIDNP in a weak magnetic field $T_1=3.8\pm0.5$ μs agrees well with the high-field value $T_1=4.4\pm0.9$ μs within the experimental accuracy. For discussion we note, that the electron spin relaxation of benzyl radicals at X-band frequency has been investigated before with the result $T_1=8.3$ μs and $T_2=2.0$ μs for the toluene solvent at 212 K (viscosity $\eta\approx2.8$ mPa s).[21] This points, as might

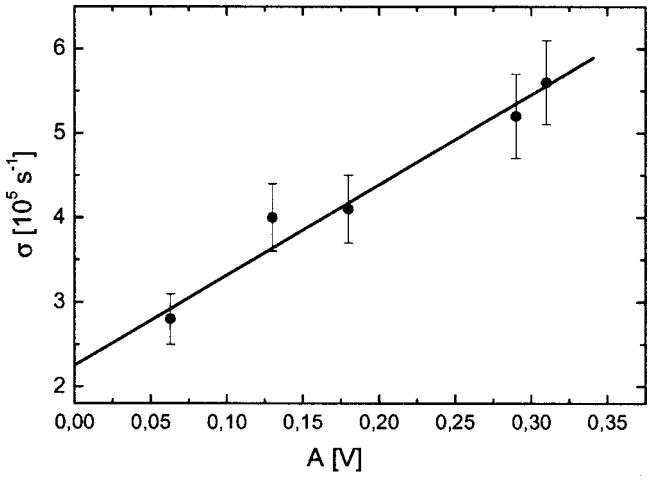

FIG. 6. Dependence of σ on A for benzyl radicals in benzene and linear regression in the region of small A.

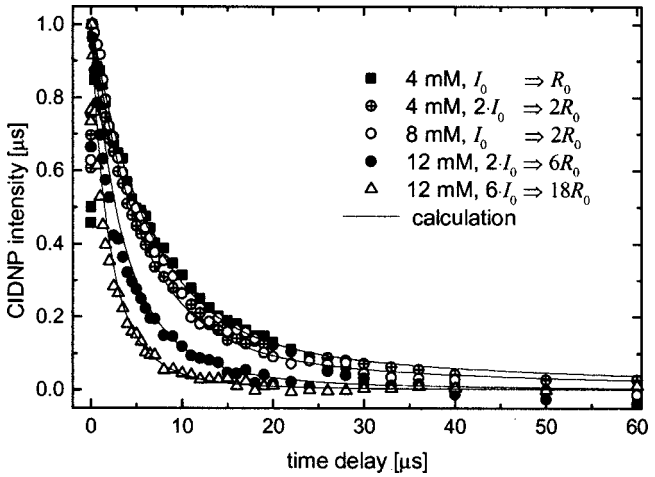

FIG. 7. SEMF CIDNP kinetics of $(CH_3)_3CH$ measured during the photolysis of DTBK at different initial concentrations of radicals R_0 in benzene. $B_1=0.5$ mT, $B_2=7.5$ mT, $\Delta\tau=5$ μs. The best fit to experimental curves has been obtained for $T_1=7.8$ μs, $\Delta P^R=1$, $\chi_1,\xi_1 \ll \chi_2=\xi_2=0.15\cdot P_0^R/R_0$, $k_{co}=8\cdot 10^5$ s^{-1}, $2kR_0=8\cdot 10^3$ s^{-1}.

have been expected for radicals with α-protons, to relaxation by the stochastic modulation of the anisotropic hyperfine interaction, slightly in the slow motional region with $(\omega_0\tau_c)^2 \approx 3$.[22] If we scale the correlation time τ_c proportional to η/T from the low temperature toluene condition to the room temperature benzene condition, then we expect the anisotropic HFI modulation to lead to $T_1 \approx 8$ μs and $T_2 \approx 6.5$ μs for the benzene solvent and RT. Our experimental result $T_1 \approx T_2 \approx 4$ μs is somewhat off the expectation and probably indicates, that at low viscosity and/or higher temperatures an additional relaxation mechanism, namely spin-rotation relaxation, comes into play. This would be in line with the findings for a variety of other small radicals.[23–25] It would also offer an explanation, why we find the relaxation in low fields to be the same or slightly faster than in the *X*-band field. According to recent theoretical work one has to expect the relaxations due to the modulations of the anisotropic HFI and the spin-rotation interaction to become slower and faster, respectively, when going to weak magnetic fields.[26,27]

B. The photolysis of di-tert.butyl ketone

Figure 7 shows the SEMF CIDNP kinetics detected during the photolysis of DTBK in benzene solution. Strong CIDNP signals were observed on the protons of the products $(CH_3)_3CH$ and $(CH_3)_2CCH_2$ of the disproportionation reaction between two tert.butyl radicals. The SEMF CIDNP kinetics was measured on the CH_3-protons of both products using $B_1=0.5$ mT and $B_2=7.5$ mT, and were found to be identical. We have measured the kinetics at different R_0 concentrations varying both laser light intensity and concentration of DTBK. As one can see from Fig. 7, at small R_0 values the kinetics depends on R_0 only very slightly, whereas for high R_0 the dependence is significant. Thus, as shown in Fig. 1(a), the kinetics at low R_0 is dominated by spin relaxation, whereas at high R_0 the chemical decay of the tert.butyl radicals contributes as well. Simulation of the kinetics measured at low R_0 yielded the spin relaxation time $T_1=(7.8\pm 0.5)$ μs. Unfortunately, the signal/noise ratio in our experiments did not allow us to measure the SEMF CIDNP kinetics at even lower R_0 where the dependence of the kinetics on R_0 is completely absent. Thus, our low field value $T_1=7.8$ μs might be slightly underestimated.

At the *X*-band field the electron spin relaxation of tert.butyl radicals is known to proceed with $T_1 \cong T_2=(3.85\pm 0.1)$ μs at RT in the benzene solvent.[20] This is about twice as fast in weak fields. The reasons for this are not yet quite clear. The anisotropies of the Zeeman and hyperfine interactions are rather small for tert.butyl radicals and should give no noticeable contributions to the spin relaxation. From EPR linewidth measurements in dependence on T/η has been concluded, that the relaxation results essentially from spin-rotation interaction.[25] However, tert.butyl radicals show a pronounced electron–nuclear cross-relaxation caused by some stochastic modulation of the isotropic HFI.[28,29] The latter mechanism should lead to a slower and the former one to a faster relaxation in weak magnetic fields.[27] The superposition of both mechanisms might well be responsible for the somewhat different spin relaxation in the strong and weak magnetic field.

C. The photolysis of di-isopropylol ketone

Figure 8 shows the SEMF CIDNP kinetics detected during the photolysis of DIPK in benzene solution using $B_1=0.5$ mT, $B_2=7.5$ mT. The kinetics shown was measured on the NMR line of acetone, formed in the disproportionation reaction of two 2-hydroxy-2-propyl radicals. The kinetics was investigated at different light intensities and found to coincide within experimental accuracy. Hence, it is determined by the spin relaxation rate in the 2-hydroxy-2-propyl radicals. Simulation using the kinetic approach yielded for the relaxation time $T_1=(2.5\pm 0.5)$ μs.

In order to determine T_1 also at *X*-band magnetic field strength we have applied the same methodology as described above for the benzyl radical. A solution of 2-hydroxy-2-methyl-propiophenone in benzene was flash-photolysed to generate the 2-hydroxy-2-propyl radicals. The relaxation

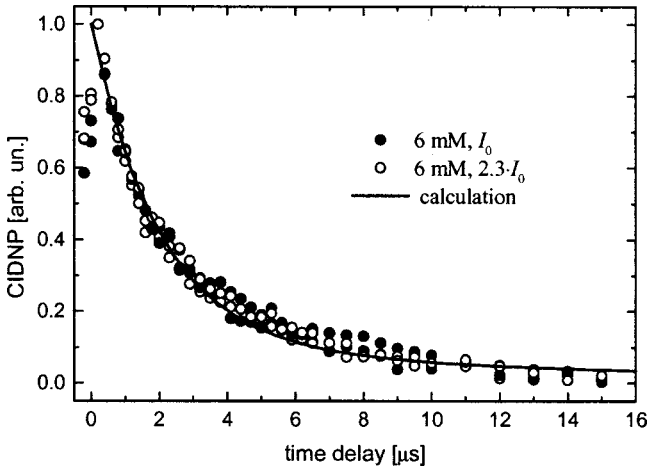

FIG. 8. SEMF CIDNP kinetics of $(CH_3)_2CO$ measured during the photolysis of DIPK at different initial concentrations of radicals R_0 in benzene. $B_1=0.5$ mT, $B_2=7.5$ mT, $\Delta\tau=5$ μs. The best fit to experimental curves has been obtained for $T_1=2.5$ μs, $\Delta P^R=1$, $\chi_1,\xi_1 \ll \chi_2=\xi_2=0.035\cdot P_0^R/R_0$, $k_{co}=4\cdot 10^7$ s^{-1}.

times $T_1 \cong T_2=(1.1\pm 0.3)$ μs were analyzed from Torrey oscillations and the EPR linewidth. One can see, that the field dependence of the relaxation of the 2-hydroxy-2-propyl radicals shows the same tendency as found above for the tert.butyl radicals. In strong magnetic fields the relaxation is roughly a factor of 2 faster than in weak ones. Both radicals have similar structures, also the 2-hydroxy-2-propyl radical shows strong indications for relaxing due to modulation of both spin-rotation and isotropic hyperfine interaction, and the above discussion for the tert-butyl radical could, mutatis mutandis, be repeated here for the 2-hydroxy-2-propyl radical.

V. CONCLUSIONS

In the present paper the method of SEMF CIDNP has for the first time been applied for studying neutral radicals in homogeneous solution. It has been shown, that the kinetics of the SEMF CIDNP is determined by both chemical reaction and spin relaxation of the intermediate radicals.

A theoretical approach has been developed for radicals with one interacting magnetic nucleus with correctly accounting for the spin dynamics and the polarization transfer, which occurs when the magnetic field is switched. It has been shown, that the kinetics of the SEMF CIDNP decays with the radical spin relaxation rate if (i) it is faster than the chemical decay of the radicals and if (ii) the contribution of the polarization formed in radical F-pairs is small. If the chemical decay of the radicals is much faster than the spin relaxation time, the SEMF CIDNP kinetics reflects the chemical kinetics of the radicals. In all other intermediate cases the kinetics is determined by both spin relaxation and chemical reaction.

For the calculation of the SEMF CIDNP kinetics in cases of more complex reaction schemes, yielding radicals containing several HFI constants, the kinetic approach developed by Vollenweider and Fischer for high-field TR CIDNP has been modified for low-field SEMF CIDNP. It has been shown that this kinetic approach reproduces well the features obtained using the exact calculation for the case of radicals with only one magnetic nucleus.

Three photochemical reactions, the photolyses of dibenzyl ketone, di-tert.butyl ketone, and di-isopropylol ketone, have been investigated experimentally using SEMF CIDNP. All the obtained features agree well with the theoretical predictions. The spin relaxation times of benzyl $[T_1=(3.8\pm 0.5)$ μs], tert.butyl $[T_1=(7.8\pm 0.5)$ μs], and 2-hydroxy-2-propyl radicals $[T_1=(2.5\pm 0.5)$ μs] have been measured in weak magnetic fields (0.5–2.0 mT) in benzene. They have been compared with those determined in a strong magnetic field (350 mT) using a time-resolved EPR technique, $T_2 \cong T_1=(4.4\pm 0.9)$ μs for benzyl, (3.85 ± 0.1) μs for tert.butyl, and (1.1 ± 0.3) μs for 2-hydroxy-2-propyl radicals. The slight differences between the low field and high field values are tentatively assigned to an interplay of several relaxation mechanisms.

It is shown that the SEMF CIDNP technique permits investigations with a time-resolution of ~20 ns of fast chemical reactions and spin relaxation times of intermediate radicals in weak magnetic fields.

ACKNOWLEDGMENTS

The authors gratefully acknowledge financial support by the Russian Foundation for Basic Research (Grant No. 02-03-32073-a), INTAS (Grant No. 99-01766), and the Swiss National Foundation for Scientific Research. E.G.B. also thanks the ''Science Support Foundation, grant for talented young researchers.''

[1] S. A. Mikhailov, P. A. Purtov, and A. B. Doktorov, Chem. Phys. **166**, 35 (1992).
[2] A. P. Parnachev, P. A. Purtov, E. G. Bagryanskaya, and R. Z. Sagdeev, J. Chem. Phys. **107**, 9942 (1997).
[3] E. G. Bagryanskaya, V. R. Gorelik, and R. Z. Sagdeev, Chem. Phys. Lett. **264**, 655 (1997).
[4] M. V. Fedin, P. A. Purtov, and E. G. Bagryanskaya, J. Chem. Phys. **111**, 5491 (1999).
[5] N. N. Lukzen and U. E. Steiner, Mol. Phys. **86**, 1271 (1995).
[6] A. B. Doktorov, Physica A **90**, 109 (1978).
[7] J.-K. Vollenweider, H. Fischer, J. Hennig, and R. Leuschner, Chem. Phys. **97**, 217 (1985).
[8] F. Jent and H. Paul, Chem. Phys. Lett. **160**, 632 (1987).
[9] H. Schuh, E. J. Hamilton, Jr., H. Paul, and H. Fischer, Helv. Chim. Acta **57**, 2011 (1974).
[10] J. K. Vollenweider and H. Paul, Int. J. Chem. Kinet. **18**, 791 (1986).
[11] M. Lehni and H. Fischer, Int. J. Chem. Kinet. **15**, 733 (1983).
[12] L. Lunazzi, K. U. Ingold, and J. C. Scaiano, J. Phys. Chem. **87**, 529 (1983).
[13] N. J. Turro, I. G. Gould, and B. H. Baretz, J. Phys. Chem. **87**, 531 (1983).
[14] Yu. P. Tsentalovich and H. Fischer, J. Chem. Soc., Perkin Trans. 2 **2**, 729 (1994).
[15] O. A. Kurnysheva, N. P. Gritsan, and Yu. P. Tsentalovich, Phys. Chem. Chem. Phys. **3**, 3677 (2001).
[16] *Landolt–Börnstein, New Series, Group 2*, edited by H. Fischer and K. H. Hellwege (Springer, Berlin, 1977), Vol. 9.
[17] H. Paul and H. Fischer, Helv. Chim. Acta **56**, 1575 (1973).
[18] J. Eichler, C. P. Herz, I. Naito, and W. Schnabel, J. Photochem. **12**, 225 (1980).
[19] A. N. Savitsky and H. Paul, Appl. Magn. Reson. **12**, 449 (1997).
[20] A. N. Savitsky, H. Paul, and A. I. Shushin, J. Phys. Chem. A **104**, 9091 (2000).

[21] R. Baer and H. Paul, Chem. Phys. **87**, 73 (1984).
[22] A. Carrington and A. D. McLachlan, *Introduction to Magnetic Resonance With Applications to Chemistry and Chemical Physics* (Harper & Row, New York, 1967).
[23] D. M. Bartels, R. G. Lawler, and A. D. Trifunac, J. Chem. Phys. **83**, 2686 (1985).
[24] B. S. Prabhananda and J. S. Hyde, J. Chem. Phys. **85**, 6705 (1986).
[25] S. N. Batchelor, B. Henningsen, and H. Fischer, J. Phys. Chem. A **101**, 2969 (1997).
[26] M. V. Fedin, P. A. Purtov, and E. G. Bagryanskaya, Chem. Phys. Lett. **339**, 395 (2001).
[27] M. V. Fedin, P. A. Purtov, and E. G. Bagryanskaya, J. Chem. Phys. (to be submitted).
[28] G.-H. Goudsmit, F. Jent, and H. Paul, Z. Phys. Chem. (Munich) **180**, 51 (1993).
[29] E. G. Bagryanskaya, G. S. Anachenko, T. Nagashima, K. Maeda, S. Milikisyants, and H. Paul, J. Phys. Chem. A **103**, 11271 (1999).